Astroparticle Physics 10 (1999) 239–252

Neutrino propagation through dense matter

Vadim A. Naumov [a,b,*], Lorenzo Perrone [b,c,1]

[a] *Laboratory of Theoretical Physics and Physics Department, Irkutsk State University, Gagarin boulevard 20, RU-664003 Irkutsk, Russia*
[b] *INFN, Sezione di Firenze, Largo Enrico Fermi 2, I-50125 Firenze, Italy*
[c] *Dipartimento di Fisica, Università degli Studi di Firenze, Firenze, Italy*

Received 27 April 1998; revised 12 June 1998; accepted 5 July 1998

Abstract

We propose a simple approach to solving the transport equation for high-energy neutrinos in dense and thick media. Illustrative results obtained from some specific models for the initial spectra of muon neutrinos and antineutrinos propagating through a normal cold medium are presented. © 1999 Elsevier Science B.V.

PACS: 05.60.+w; 13.15.+g; 14.60.Lm
Keywords: Transport theory; Neutrino interactions

1. Introduction

During their passage through a medium, high-energy neutrinos and antineutrinos are absorbed and lose their energy (and therefore regenerate) due to charged and neutral current interactions. In a normal *cold* medium, like the interior of the Earth or a star, these interactions consist of νN ($\overline{\nu}N$) and νe ($\overline{\nu}e$) collisions. In more exotic media such as *hot* galactic haloes filled with massive neutrinos [1] and at super-high energies $\nu\overline{\nu}$ annihilations become important. As a result, the spectrum of extraterrestrial neutrinos, in their passage from source to detector, is transformed first in the medium surrounding the source, then in the cosmic backgrounds, and finally in the Earth. For media with thicknesses in excess of several neutrino interaction lengths λ_ν this transformation becomes dramatic. Therefore, a detailed study of neutrino transport through thick media, taking into account neutrino regeneration, is one of the key elements in ultra-high energy (UHE) neutrino astrophysics.

In the last few years, several projects have been proposed [2] for the search of UHE extraterrestrial neutrinos by detecting Čerenkov radiation from muons and electromagnetic or hadronic showers produced by neutrinos in a transparent detector medium (water or ice) or in rock surrounding the detector. Two of these projects, AMANDA and the Baikal neutrino telescope, are already operational; two others, ANTARES and NESTOR, are under development. The ultimate, still remote aim of these projects is to make up a huge observatory

* Corresponding author; e-mail: naumov@api.isu.runnet.ru, naumov@fi.infn.it
[1] E-mail: perrone@fi.infn.it

PII S0927-6505(98)00046-2

with a sensitive volume of up to 1 km^3 for the studying of UHE neutrino astrophysics and the search for particle physics beyond the Standard Model [3,4]. A further increase of the sensitivity of underwater/ice neutrino telescopes would be possible with techniques based upon hydroacoustic and radiowave detection of neutrino-induced showers [5]. Recently, it has been shown [6] that the future (ground-based) Pierre Auger Observatory [7] also has the potential to detect neutrinos of energies in the multi-EeV range through near-horizontal air showers. Even more futuristic projects, such as SOCRAS, MASS, OWL, and the "Airwatch form Space" Mission [8], are now under discussion. They are based on the "Space-Airwatch" method of detecting and identifying giant Auger showers by means of the fluorescence they induce in atmospheric nitrogen observed from outer space [9]. This method provides the possibility of studying cosmic rays, including gammas and neutrinos, with energies above 10 EeV, by monitoring a fiducial area of 10^6–10^7 km^2 with orbiting detector(s). Evidently, the problem of neutrino transport through matter will grow in importance with an increase in neutrino energy ranges accessible to observation.

The effect of neutral current on the electron and muon (anti)neutrino absorption and regeneration was investigated for the first time in Ref. [10] for the case of initial spectra following a power-law. It was shown that, within a simple approximation, the neutrino absorption length Λ_ν exceeds the interaction length, λ_ν, as in the case of hadronic cascades. As a consequence, the regeneration correction to the neutrino penetration coefficient grows exponentially with depth and energy.

In Ref. [11], the effect of neutral currents was studied for the spectrum of neutrinos originating from annihilation of massive neutralinos captured in the solar core which do not follow a power-law and for the spectrum of AGN neutrinos penetrating the Earth. In their calculations, the authors used the method of successive generations and direct Monte Carlo simulation. In particular, it was shown, that the regeneration due to neutral currents essentially affects the flux of the neutrino-induced upgoing muons. For example, in the case of AGN neutrinos, the yield of vertical muons with energies $\geqslant$ 100 TeV per one neutrino with energy of 20 PeV (60 PeV) is roughly 100 (1000) times larger than that estimated neglecting the correction due to neutrino regeneration. Clearly, the effect diminishes after integration of the muon yield over the neutrino spectrum, but it increases fast when increasing the muon energy threshold.

Using a simple model for νN cross sections, it recently was demonstrated analytically [12] that the approximation of Ref. [10] has a limited range of applicability even for power-law initial spectra. Owing to the strong energy dependence of the total νN cross sections, the effective absorption length, Λ_ν, becomes depth-dependent. As a consequence, the neutrino penetration coefficient, as a function of depth, does not follow a simple exponential law. A similar situation is well-known in muon transport theory (see, e.g., Ref. [13]), but for muons the magnitude of this effect becomes very small at high energies (above $\sim$ 10 TeV) [2], while for neutrinos it grows with energy and depth.

The goal of this work is to provide an elementary analytical method for the precise calculation of energy spectra of high-energy neutrinos after their propagation through a dense medium of *any* thickness. The method of Ref. [12] was developed for simplified models of the initial neutrino spectrum and the νN cross sections (differential and total). Our approach does not require simplifications and is applicable to initial spectra and cross sections of any form. In Sections 2 and 3, we will only consider the decreasing continuous initial spectra most interesting for UHE neutrino astrophysics. However, the main idea of the method can also be extended to a monoenergetic spectrum (see Appendix A). This extension may be useful, in particular, for simulating single neutrino events for a neutrino experiment. Furthermore, the method makes no assumptions specific to neutrinos and can be straightforwardly extended to the problem of transport of high-energy particles other than neutrinos (e.g., cosmic-ray nucleons and muons in the atmosphere [14]).

In this paper, we will only consider media that are sufficiently dense to neglect the charged-current induced regeneration processes. To elucidate this point, let us take a brief look at the main features of the neutrino

[2] Since the differential cross sections for the muon radiative processes are energy-independent in the limit of complete screening and the muon photonuclear cross section grows with energy only logarithmically.

transport in low-density media.

Under certain conditions, neutrinos may transform, changing energy and/or flavour via processes like $\overline{\nu}_e e^- \to \overline{\nu}_\ell \ell^-$ or $\nu_\ell e^- \to \nu_e \ell^-$ $(\ell = e, \mu, \tau)$, owing to the production and decay of unstable hadrons or, in the abovementioned massive-neutrino haloes, through reaction chains like $\nu_\mu \overline{\nu}_\tau \to \mu^- \tau^+$, $\tau^+ \to \overline{\nu}_\tau X$, etc. In particular, the neutrino regeneration in hadronic cascades can play a role if the column depth of the medium exceeds $\lambda_\nu(E)$, while the average density is sufficiently low [3], namely,

$$\langle \rho \rangle \lesssim \rho_h^0 \left[\frac{\lambda_h^{\text{inel}}(E_h)}{45 \text{ g/cm}^2} \right] \left[\frac{1 \text{ PeV}}{E_h} \right].$$

Here $\lambda_h^{\text{inel}}(E_h)$ is the inelastic scattering length [4] for a hadron h of energy $E_h = \xi_h E$ at production, ξ_h is the average fraction of the incident neutrino energy E carried by the hadron; $\rho_h^0 = 0.8 \times 10^{-8}$, 6×10^{-8}, 1.4×10^{-8} g/cm^3 for $h = \pi^\pm$, $K^\pm$, K_L^0, respectively, and $\rho_h^0 \sim 10^{-2}$ g/cm^3 for $h = D^\pm, D^0, \overline{D}^0$ and $\Lambda_c^\pm$. Generally, this mechanism is not-too-effective because ξ_h is very small. However, it becomes important for flat neutrino spectra, like ones expected from topological defects.

The charged-current induced reaction chains $\nu_\mu N \to \mu^- X$, $\mu^- \to \nu_\mu \overline{\nu}_e e^-$ and $\overline{\nu}_\mu N \to \mu^+ X$, $\mu^+ \to \nu_\mu \nu_e e^+$ are much more effective if

$$\langle \rho \rangle \lesssim 6.4 \times 10^{-7} \left[\frac{2.5 \times 10^{-6} \text{ cm}^2 \text{g}^{-1}}{b_\mu(E_\mu)} \right] \left[\frac{1 \text{ PeV}}{E_\mu} \right] \frac{\text{g}}{\text{cm}^3}, \tag{1}$$

where b_μ, being the muon fractional energy loss due to radiative and photonuclear interactions, is a slowly varying function of the muon energy $E_\mu = \xi_\mu E$ with $\xi_\mu \sim 1$. Elementary considerations suggest that under the condition (1) even very thick layers of matter never become opaque to ν_μ and $\overline{\nu}_\mu$.

Let us note that the form of the density distribution and the composition of the medium also affect the neutrino yields from the decay of hadrons and muons. As a result, the regeneration effect may be very different for neutrino beams penetrating the same *nonuniform* medium in different directions.

As it was pointed out recently [16], UHE tau neutrinos and antineutrinos effectively regenerate (losing energy) even in rather dense media, through the charged-current reaction chain $\nu_\tau N \to \tau X$, $\tau \to \nu_\tau X$. Indeed, the corresponding "critical" density can be roughly estimated as

$$2 \times 10^4 \left[\frac{10^{-8} \text{ cm}^2 \text{g}^{-1}}{b_\tau(E_\tau)} \right] \left[\frac{1 \text{ PeV}}{E_\tau} \right] \frac{\text{g}}{\text{cm}^3} \qquad (E_\tau = \xi_\tau E \sim E).$$

The Earth is therefore effectively transparent for ν_τ and $\overline{\nu}_\tau$ at energies up to 1–10 EeV. This fact is very profitable for future experiments with underwater neutrino telescopes (e.g., detecting ν_τ events from astrophysical neutrino oscillations at energies $\gtrsim 1$ PeV [17]), and especially for UHE neutrino experiments based on the "Space-Airwatch" method. Indeed, extraterrestrial tau neutrinos will produce detectable upgoing showers from the whole lower semisphere, whereas showers produced by electron and muon UHE neutrinos can be detected from outer space only within a narrow solid angle around the horizontal directions.

Mathematically, the consideration of processes that change the neutrino flavour and of neutrino energy loss through creation and decay of short-lived particles leads to a system of transport equations that explicitly include the density distribution along the neutrino beam path. The extension of our method to a general system is not straightforward and demands additional assumptions specific to the task. However, the case when these contributions may be treated as corrections presents no special problem. Since this case is rather

[3] A Thorne–Żytkow object [15] (a neutron star inside a supergiant core) is a good example of such a medium. Regeneration due to neutrinoproduction and decay of charmed particles may be of some effect for neutrinos propagating through the solar atmosphere.

[4] $\lambda_h^{\text{inel}} = 45$ g/cm^2 is the typical value for a hydrogen–helium target.

common (neutrino production in the ν-induced hadronic cascades is a typical example), we briefly describe the corresponding trivial generalization in Appendix B.

To avoid technical complications, in the main text, we will neglect the (standard and hypothetical) flavour-changing neutrino interactions[5] and will use the simplest "standard" scenario for neutrino propagation described by a *single* transport equation. We will consider sufficiently high energies in order to allow us to neglect the thermal velocities of the scatterers in the target medium and to simplify to one-dimensional theory. As an illustration, we will discuss results obtained with some specific models for the initial spectra of muon neutrinos and antineutrinos propagating through a normal cold medium (Section 3).

2. Method for solution of the neutrino transport equation

Let $F_\nu(E,x)$ be the differential energy spectrum of neutrinos at a column depth x in a medium defined by

$$x = \int_0^L \rho(L')\,\mathrm{d}L',$$

where $\rho(L)$ is the density of the medium at the distance L from the boundary measured along the neutrino beam path. Then, neglecting the flavour-changing and charged-current induced regeneration processes mentioned in the introduction, one can derive the one-dimensional transport equation

$$\frac{\partial F_\nu(E,x)}{\partial x} = \frac{1}{\lambda_\nu(E)}\left[\int_0^1 \Phi_\nu(y,E)\,F_\nu\left(\frac{E}{1-y},x\right)\frac{\mathrm{d}y}{1-y} - F_\nu(E,x)\right], \tag{2}$$

with the boundary condition $F_\nu(E,0) = F_\nu^0(E)$. Here, $\lambda_\nu(E)$ is the neutrino interaction length defined by

$$\frac{1}{\lambda_\nu(E)} = \sum_T N_T \sigma_{\nu T}^{\mathrm{tot}}(E),$$

where N_T is the number of scatterers T in 1 g of the medium, $\sigma_{\nu T}^{\mathrm{tot}}(E)$ is the total cross section for the νT interactions, and the sum is over all scatterer types $(T = N, e, \ldots)$. The "regeneration function" $\Phi_\nu(y,E)$ is defined by

$$\sum_T N_T \frac{\mathrm{d}\sigma_{\nu T\to\nu X}(y,E_y)}{\mathrm{d}y} = \Phi_\nu(y,E)\sum_T N_T\sigma_{\nu T}^{\mathrm{tot}}(E),$$

where $\mathrm{d}\sigma_{\nu T\to\nu X}(y,E)/\mathrm{d}y$ is the differential cross section for the inclusive reaction $\nu T \to \nu X$ (with E the initial neutrino energy and y the fraction of energy lost) and $E_y \equiv E/(1-y)$.

Let us define the effective absorption length $\Lambda_\nu(E,x)$ by

$$F_\nu(E,x) = F_\nu^0(E)\exp\left[-\frac{x}{\Lambda_\nu(E,x)}\right]. \tag{3}$$

As is evident from Eq. (2), $\Lambda_\nu(E,x) > \lambda_\nu(E)$ for any finite E and x. Therefore

$$\Lambda_\nu(E,x) = \frac{\lambda_\nu(E)}{1 - Z_\nu(E,x)}, \tag{4}$$

[5] As well as the effects of possible neutrino flavour mixing.

where $Z_\nu(E,x)$ is a positive function (we will call it the Z factor in analogy with the hadronic cascade theory) which contains the complete information about the neutrino kinetics in matter.

Substituting Eqs. (3) and (4) into Eq. (2) and integrating by parts, it is easy to derive the integral equation for the Z factor:

$$Z_\nu(E,x) = \frac{1}{x}\int_0^x\int_0^1 \eta_\nu(y,E)\,\Phi_\nu(y,E)\exp\left[-x' D_\nu(E,E_y,x')\right]\mathrm{d}x'\,\mathrm{d}y, \tag{5}$$

with

$$D_\nu(E,E_y,x) = \frac{1-Z_\nu(E_y,x)}{\lambda_\nu(E_y)} - \frac{1-Z_\nu(E,x)}{\lambda_\nu(E)}$$

and

$$\eta_\nu(y,E) = \frac{F_\nu^0(E_y)}{F_\nu^0(E)\,(1-y)}.$$

We dwell on Eq. (5). Although nonlinear, it is more suitable for an iteration solution than Eq. (2), considering the smallness of the Z factor and (what is more important) the model-independent feature of the regeneration function $\Phi_\nu(y,E)$, namely, its sharp maximum at $y=0$.

In this section, we assume that the initial spectrum $F_\nu^0(E)$ is a continuous function decreasing at very high energies sufficiently fast that $0 \leqslant \eta_\nu(y,E) < \infty$ for any E and $0 \leqslant y \leqslant 1$. Actually, the neutrino spectra of interest for UHE neutrino astrophysics decrease everywhere so fast that $0 \leqslant \eta_\nu(y,E) < 1$ for any E and $y > 0$.

First we will look at the case of thin absorbers. One readily sees

$$Z_\nu(E,0) = \int_0^1 \eta_\nu(y,E)\,\Phi_\nu(y,E)\,\mathrm{d}y \equiv Z_\nu^0(E).$$

Usually the approximation $Z_\nu(E,x) = Z_\nu^0(E)$ is utilized in studying the propagation of the muon neutrino through matter (see, e.g., Refs. [10,3] and references therein). However, at sufficiently high energies this approximation becomes too rough even for "shallow" (as compared to λ_ν) depths. Indeed, taking into account the $\mathcal{O}(x/\lambda_\nu)$ correction yields

$$Z_\nu(E,x) \approx Z_\nu^0(E) - \frac{x\Delta_\nu^1(E)}{2\lambda_\nu(E)},$$

where

$$\Delta_\nu^1(E) = -\lambda_\nu(E)\left[\frac{\partial Z_\nu(E,x)}{\partial x}\right]_{x=0} = \int_0^1 \eta_\nu(y,E)\,\Phi_\nu(y,E)\left\{[1-Z_\nu^0(E_y)]\frac{\lambda_\nu(E)}{\lambda_\nu(E_y)} - [1-Z_\nu^0(E)]\right\}\mathrm{d}y.$$

Thus, the approximation $Z_\nu \approx Z_\nu^0$ can only be valid for

$$\frac{x}{\lambda_\nu(E)} \ll \frac{2Z_\nu^0(E)}{|\Delta_\nu^1(E)|}.$$

Generally, the function $\Delta_\nu^1(E)$ is not small in comparison with $Z_\nu^0(E)$. This can be demonstrated with the simple model adopted in Ref. [12]. The authors of Ref. [12] assumed that $\Phi_\nu = \Phi_\nu(y)$ is an energy-independent function, $\lambda_\nu(E) \propto E^{-\beta}$ and $F_\nu^0(E) \propto E^{-(\gamma+1)}$ with energy-independent positive β and γ. All these assumptions are far from realistic but may have a physical sense at ultra-high energies. For example, owing to the νN interactions, β is a monotonically decreasing function of E changing from about 1 at $E \lesssim 1$ TeV to about 0.4 at $E \gtrsim 1$ PeV [18] (cf. Ref. [19]); the function $\Phi_\nu(y,E)$ strongly varies with E at all energies, but for $E \gtrsim 1$ PeV it may be roughly approximated by a scaling function (see Fig. 1 in Section 3) [6]. In this model, both Z_ν^0 and Δ_ν^1 are energy-independent:

$$Z_\nu^0 = \int_0^1 (1-y)^\gamma \Phi_\nu(y)\,\mathrm{d}y, \qquad \Delta_\nu^1 = (1-Z_\nu^0)\int_0^1 (1-y)^\gamma [(1-y)^{-\beta}-1]\Phi_\nu(y)\,\mathrm{d}y.$$

Evidently, Δ_ν^1 can be much larger than Z_ν^0 for a sufficiently hard initial neutrino spectrum (small γ) [7].

It is not a hard task to derive the $\mathcal{O}((x/\lambda_\nu)^k)$ corrections for $k = 2, 3, \ldots$, but as a result we will get an asymptotic expansion with coefficient functions, $\Delta_\nu^k(E)$, increasing fast with k. The range of applicability of this expansion proves to be very limited and decreases fast with increasing energy.

Now, let us consider a way to solve Eq. (5) for any depth and energy. We will use an iteration algorithm. Let n label the iteration number. Then we define

$$D_\nu^{(n)}(E,E_y,x) = \frac{1-Z_\nu^{(n)}(E_y,x)}{\lambda_\nu(E_y)} - \frac{1-Z_\nu^{(n)}(E,x)}{\lambda_\nu(E)} \tag{6}$$

and

$$Z_\nu^{(n+1)}(E,x) = \frac{1}{x}\int_0^x\int_0^1 \eta_\nu(y,E)\,\Phi_\nu(y,E)\exp[-x' D_\nu^{(n)}(E,E_y,x')]\,\mathrm{d}x'\,\mathrm{d}y. \tag{7}$$

Due to the abovementioned sharp maximum of $\Phi_\nu(y,E)$, the main contribution to the integral over y on the right-hand side of Eq. (7) comes from the region around the lower limit. But $D_\nu(E,E_y,x) \to 0$ as $y \to 0$ and thus the algorithm is robust in respect to choosing the zero approximation. The simplest choice is $Z_\nu^{(0)}(E,x) = 0$. Therefore

$$D_\nu^{(0)}(E,E_y,x) = \frac{1}{\lambda_\nu(E_y)} - \frac{1}{\lambda_\nu(E)} \equiv \mathcal{D}_\nu(E,E_y). \tag{8}$$

Formally the algorithm (6)–(8) is applicable for arbitrarily decreasing initial spectra. It is however clear that the softer the initial spectrum, the better the convergence of the algorithm. In the next section, we show that the algorithm converges very fast for realistic initial spectra and has no restrictions in depth or energy. Moreover, even the first approximation,

$$Z_\nu^{(1)}(E,x) = \int_0^1 \eta_\nu(y,E)\,\Phi_\nu(y,E)\left[\frac{1-\mathrm{e}^{-x\mathcal{D}_\nu(E,E_y)}}{x\mathcal{D}_\nu(E,E_y)}\right]\mathrm{d}y, \tag{9}$$

proves to be quite accurate. It has the correct asymptotic behaviour both in energy and depth and it can thus be used for an analytical or numerical evaluation of the Z factor with a not-too-big error.

[6] However, as Fig. 1 suggests, the specific parametrization used in Ref. [12], $\Phi_\nu(y) \propto (\mathrm{const}+y)^{-1}$, is too rough even at super-high energies.

[7] In real cases, $\Delta_\nu^1(E)$ is nevertheless finite because any physical spectrum $F_\nu^0(E)$ has a cutoff at some finite energy E_{cut} and therefore $\eta_\nu(y,E) = 0$ at $y \geqslant 1 - E/E_{\mathrm{cut}}$.

Assuming that $\lambda_\nu(E)$ is a decreasing function [8] and therefore $\mathcal{D}_\nu(E, E_y) > 0$ for $y > 0$, one can prove that
$Z_\nu^{(1)}(E, x) \leqslant Z_\nu^0(E)$ at any E and $x \geqslant 0$, and
$Z_\nu^{(1)}(E, x) \to 0$ as $x \to \infty$ at any E.
The latter means that the neutrino regeneration due to the inclusive reactions $\nu T \to \nu X$ becomes negligible at sufficiently large depths. This conclusion remains true for the exact solution of Eq. (5), under rather general assumptions about the behaviour of the initial neutrino spectrum and cross sections.

3. Numerical illustration and discussion

In the following we will only consider muon neutrinos and antineutrinos propagating through a normal medium. However, the results that follow also hold for electron neutrinos. In this calculation, we will neglect neutrino scattering off electrons (thus we exclude electron antineutrinos from our consideration) as well as the neutrino regeneration in the ν-induced cascades. In order to simplify further, we shall deal with an isoscalar medium neglecting nuclear effects.

To calculate the differential $\nu_\mu N$ and $\overline{\nu}_\mu N$ cross sections, we use the approach of Ref. [18] based on the renormalization-group-improved parton model and new experimental information about the quark structure of the nucleon. Various versions of different sets of parton density functions $q(\hat{x}, Q^2)$ are now collected in the large CERN program library PDFLIB [20]; they can be simply accessed by setting a few parameters to choose a desired version. In this calculation, following Ref. [18], we selected the third version of the CTEQ collaboration model [21] for the next-to-leading order (NLO) quark distributions in the deep-inelastic scattering factorization scheme. The Q^2 evolution is obtained numerically using the NLO Gribov–Lipatov–Altarelli–Parisi equations from the initial value $Q_0^2 = 2.56$ GeV^2. The CTEQ3 distributions are particularly suitable for our aims because the numerical evolution is provided for very low Bjorken $\hat{x}$. Unfortunately, at high energies the uncertainty resulting from this extrapolation may be rather large. According to the most recent analysis [19], for neutrino energies up to ~ 10 PeV, all the standard sets of parton distribution functions yield very similar cross sections. However, at higher energies, cross sections become sensitive to the behaviour of parton distributions at $\hat{x} \ll 10^{-4}$, where there are no direct experimental constraints. Reasoning from the most extreme variations, the authors conclude that at $E = 100$ EeV the uncertainty reaches a factor of $2^{\pm 1}$.

It was calculated in Ref. [22] that the QED radiative corrections (in leading logarithmic approximation) essentially modify the UHE single-differential cross section $\mathrm{d}\sigma_{\nu N \to \mu X}/\mathrm{d}y$, especially at low y, while they are almost negligible for the total cross section. In the present calculation, we neglect the radiative corrections, considering that the mentioned uncertainty in the parton density functions at very low $\hat{x}$ is the dominant source of uncertainty in the differential cross sections. It should be noted here that possible uncertainties in the NC cross section, $\mathrm{d}\sigma_{\nu N \to \nu X}/\mathrm{d}y$, at low y can affect the Z factors, but they are essentially cancelled in the effective absorption lengths, $\Lambda_\nu(E, x)$.

The total cross sections for CC and NC inelastic scattering of muon neutrinos and antineutrinos off an isoscalar nucleon are shown in Fig. 1 as the solid (ν_μ) and dashed ($\overline{\nu}_\mu$) curves. Fig. 2 shows the regeneration functions $\Phi_{\nu_\mu}(y, E)$ (solid curves) and $\Phi_{\overline{\nu}_\mu}(y, E)$ (dashed curves) versus y for several values of E (10^3 to 10^{12} GeV).

At all energies, our calculation for the cross sections agrees with the result of Ref. [18] within a few-percent accuracy; the insignificant difference near the resonance region ($< 4\%$) is due mainly to differences in the adopted values for the electroweak parameters (W/Z boson masses, t quark mass, Weinberg angle, etc.) [9] and, at the highest energies, due to the top sea contribution neglected in Ref. [18]. As one can see from the figures, the ν_μ and $\overline{\nu}_\mu$ scatterings become indistinguishable for $E \gtrsim 1$ PeV.

[8] For a normal medium, this is true for all neutrino flavours except $\overline{\nu}_e$ (see Ref. [18]).
[9] In our calculation, all these parameters were updated according to the current PDG data [23].

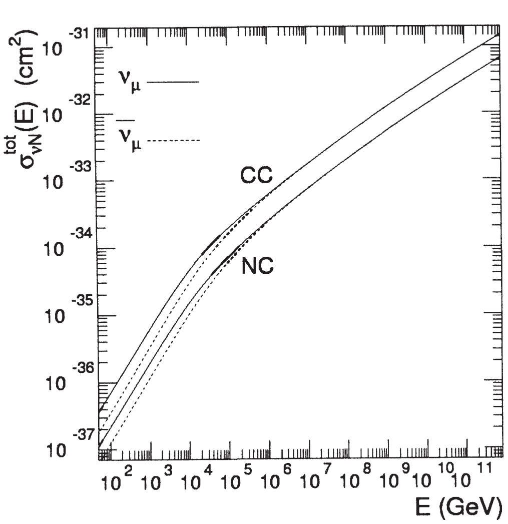

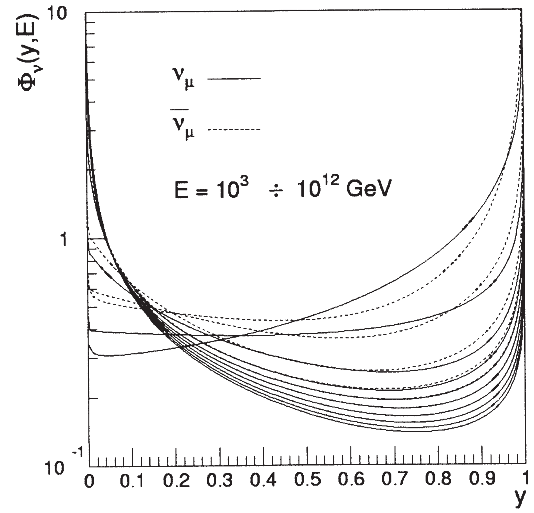

Fig. 1. Total charged and neutral current $\nu_\mu N$ and $\overline{\nu}_\mu N$ cross sections versus energy.

Fig. 2. Regeneration functions $\Phi_{\nu_\mu}(y,E)$ and $\Phi_{\overline{\nu}_\mu}(y,E)$ versus y for $E = 10^k$ GeV ($k = 3, 4, \ldots, 12$ from top to bottom).

We use the following model for the initial neutrino spectrum:

$$F_\nu^0(E) = K\left(\frac{E_0}{E}\right)^{\gamma+1}\left(1+\frac{E}{E_0}\right)^{-\alpha}\phi\left(\frac{E}{E_{\rm cut}}\right), \tag{10}$$

where K, γ, α, E_0, and $E_{\rm cut}$ are parameters and $\phi(t)$ is a function equal to 0 at $t \geqslant 1$ and 1 at $t \ll 1$. Varying the parameters in Eq. (10), we can approximate many models for the neutrino fluxes expected from the known astrophysical sources. Technically, the function $\phi(t)$ serves to avoid an extrapolation of the cross sections to the extremely-high energy region for which our knowledge of the parton density functions is limited. For realistic values of the parameters γ, α, and E_0, the explicit form of $\phi(t)$ is of no importance as long as one is interested in the energy range $E \ll E_{\rm cut}$. In fact, $\phi(t)$ may be treated as a real physical cutoff of the spectrum determined by the energetics of a neutrino source or by neutrino interactions with cosmic background. In the present calculations, we adopt (without serious physics arguments) $\phi(t) = 1/[1+\tan(\pi t/2)]$ $(t < 1)$ and $E_{\rm cut} = 3\times 10^{10}$ GeV.

Fig. 3 shows the energy dependence of the Z factors, $Z_{\nu_\mu}(E,x)$ (solid curves) and $Z_{\overline{\nu}_\mu}(E,x)$ (dashed curves) for various depths, from $x = 0$ to $x = x_\oplus$ (where $x_\oplus \approx 1.1\times 10^{10}$ g/cm^2 is the column depth of the Earth along the diameter), for the initial spectra (10) calculated with $\gamma = 0.5$, $\alpha = 1$ (a), $\gamma = 1$, $\alpha = 0.5$ (b), $\gamma = 1.5$, $\alpha = 0.5$ (c), and $\gamma = 2$, $\alpha = 1$ (d). In all cases we used $E_0 = 1$ PeV.

The calculations were made in the fourth order of the iteration procedure described in Section 2. For all spectra under discussion, for 10 GeV $\leqslant E \leqslant 10^{10}$ GeV and $0 \leqslant x \leqslant x_\oplus$, the maximum difference between $Z_\nu^{(1)}(E,x)$ and $Z_\nu^{(2)}(E,x)$ is about 4%; the value $|Z_\nu^{(3)}/Z_\nu^{(2)} - 1|$ is less than 2×10^{-3}, and $|Z_\nu^{(4)}/Z_\nu^{(3)} - 1|$ is less than the precision of the numerical integration and interpolation (about 10^{-5}) adopted in our calculations. After tests with many models for the initial spectrum (including atmospheric neutrino spectra from Ref. [24]), we conclude that the convergence of the algorithm is very good and that even the first approximation, $Z_\nu^{(1)}(E,x)$, has an accuracy which is quite sufficient for the majority of applications of the theory.

As is clear from Fig. 3, the shape of the Z factors strongly depends on the initial spectrum. This is a positive fact for neutrino astronomy since, at least in principle, it enables one to reconstruct the initial neutrino spectrum from the measured energy spectrum and the angular distribution of neutrino induced muon events in a neutrino telescope.

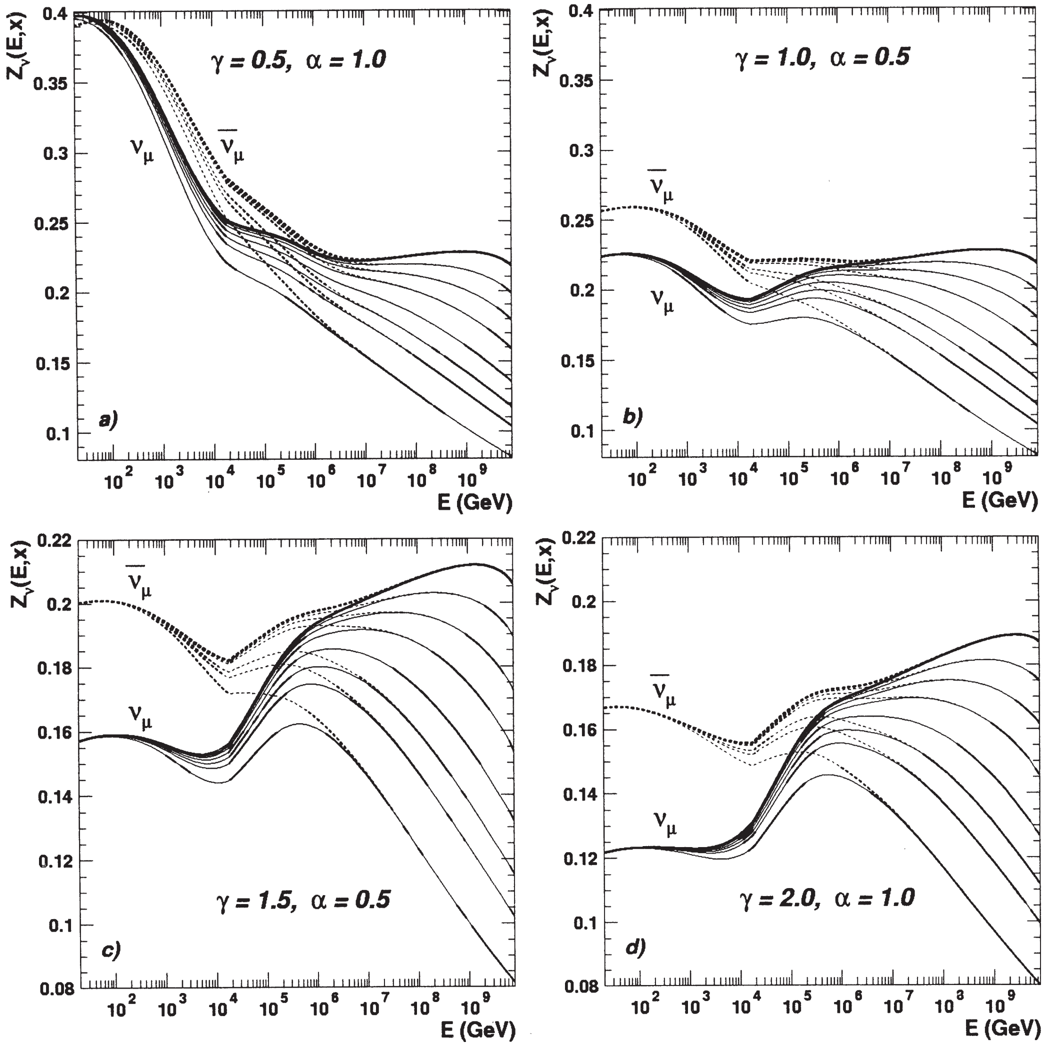

Fig. 3. Z factors, $Z_{\overline{\nu}_\mu}(E,x)$ and $Z_{\nu_\mu}(E,x)$ versus energy for the initial spectra (10), calculated with four different sets of γ and α and with E_0 = 1 PeV for depths $x = x_\oplus/k$ ($k = 1, 2, 3, 5, 10, 20, 50$ from bottom to top) and $x = 0$ (the largest Z factors).

At comparatively low energies (except for unrealistically hard spectra like the one used in Fig. 3a), the Z factors for antineutrinos exceed those for neutrinos. Considering the inequality $\lambda_{\overline{\nu}_\mu}(E) > \lambda_{\nu_\mu}(E)$, one can conclude that

$$\Lambda_{\overline{\nu}_\mu}(E,x) > \Lambda_{\nu_\mu}(E,x)$$

for any depth. In the multi-PeV energy range and above, the Z factors (and effective absorption lengths) are identical for ν_μ and $\overline{\nu}_\mu$. The difference between the shapes of $Z_{\nu_\mu}(E,x)$ and $Z_{\overline{\nu}_\mu}(E,x)$ is almost depth-independent and becomes more important for steep initial spectra. This behaviour may be understood from an analysis of the shapes of the total cross sections and regeneration functions for ν_μ and $\overline{\nu}_\mu$ (Figs. 1 and 2).

At any fixed energy, the Z factors monotonically decrease with increasing depth and the inequality $Z_\nu(E,x) < Z_\nu^0(E)$ takes place for any $x > 0$. This effect leads to a significant decrease of the neutrino event rates in comparison with those estimated in the "standard" approximation $Z_\nu \approx Z_\nu^0$; the latter only works at low

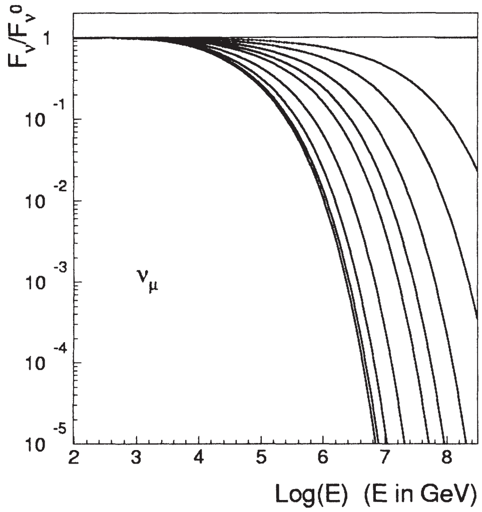

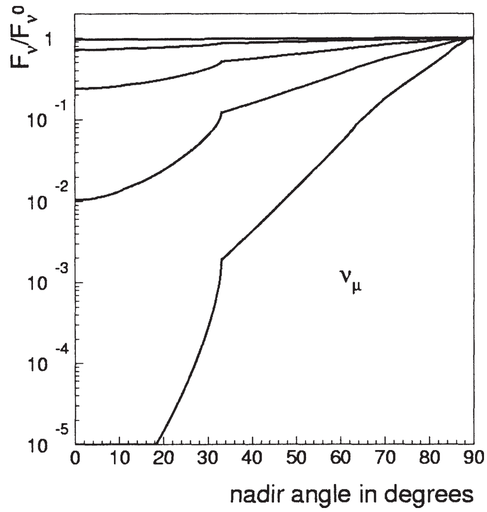

Fig. 4. Neutrino penetration coefficient in the Earth for the quasi-power-law initial spectrum with $\gamma = 0.7$ as a function of E at fixed ϑ (0° to 90° from bottom to top with steps of 10°).

Fig. 5. Neutrino penetration coefficient in the Earth for the quasi-power-law initial spectrum with $\gamma = 0.7$ as a function of ϑ for $E = 10^k$ GeV ($k = 3, 4, \ldots, 7$ from top to bottom).

energies, when the shadow effect is by itself small (that is when the medium is almost transparent for neutrinos). Although these conclusions were derived from particular models for the initial neutrino spectrum, cross sections, and medium, they are actually highly general and model-independent.

In Figs. 4 and 5, we present the penetration coefficient, $\exp[-x/\Lambda_\nu(E,x)]$, in the Earth for muon neutrinos with the initial spectrum (10) calculated with $\gamma = 0.7$ and $\alpha = 0$ ("quasi-power-law" spectrum). The results are presented as a function of E for several nadir angles (ϑ) (Fig. 4) and as a function of ϑ for several values of E (Fig. 5).

To evaluate the depth x as a function of ϑ, we use the density profile of the Earth, $\rho(L)$, given from the "Preliminary Reference Earth Model" (see Ref. [18]). The kinks in Fig. 5 are due to the layered structure of the Earth.

Acknowledgements

We wish to acknowledge very helpful and constructive discussions with Bianca Monteleoni whose encouragement stimulated this work. We also thank Ina Sarcevic for providing us with the Fortran code that was used to test our calculations of the νN cross sections. We acknowledge the hospitality of INFN, Sezione di Firenze, where this research was performed. The work of V.N. was supported in part by the Ministry of General and Professional Education of Russian Federation, within the framework of the program "Universities of Russia – Basic Researches", grant No. 728.

Appendix A. Monochromatic initial spectrum

Let us consider the initial "spectrum" of the form $\delta(E - E_0)$ with the parameter E_0. In this appendix, we will show how this monochromatic spectrum transforms at depth x in a medium. Let us denote the transformed spectrum by $G_\nu(E_0;E,x)$. This function must satisfy Eq. (2) and simple considerations suggest the following ansatz:

$$G_\nu(E_0;E,x) = \left[\delta(E-E_0) + \frac{\theta(E_0-E)}{E}\psi_\nu(E_0;E,x)\right]\mathrm{e}^{-x/\lambda_\nu(E_0)}, \tag{A.1}$$

where the term with δ function describes absorption of initial ("parent") neutrinos of energy E_0 and the next term – the creation and propagation of secondary neutrinos with energy $E < E_0$. Substituting Eq. (A.1) into Eq. (2) yields

$$\frac{\partial\psi_\nu(E_0;E,x)}{\partial x} = \frac{1}{\lambda_\nu(E)}\left[\int_0^{y_0}\Phi_\nu(y,E)\,\psi_\nu(E_0;E_y,x)\,\mathrm{d}y + \Omega_\nu(E,E_0)\right] + \mathcal{D}_\nu(E,E_0)\,\psi_\nu(E_0;E,x),$$
$$\psi_\nu(E_0;E,0) = 0, \tag{A.2}$$

where $\Omega_\nu(E,E_0) = (1-y_0)\Phi_\nu(y_0,E)$, $y_0 \equiv 1 - E/E_0 < 1$, and $\mathcal{D}_\nu(E,E_0)$ is defined by Eq. (8).

Let us seek the solution to Eq. (A.2) in the form

$$\psi_\nu(E_0;E,x) = \Omega_\nu(E,E_0)\int_0^x \exp\left[\int_{x'}^x \frac{\mathrm{d}x''}{\mathcal{L}_\nu(E_0;E,x'')}\right]\frac{\mathrm{d}x'}{\lambda_\nu(E)}, \tag{A.3}$$

$$\frac{1}{\mathcal{L}_\nu(E_0;E,x)} = \frac{1}{\lambda_\nu(E_0)} - \frac{1-\mathcal{Z}_\nu(E_0;E,x)}{\lambda_\nu(E)}, \tag{A.4}$$

with $\mathcal{Z}_\nu(E_0;E,x)$ an unknown positive function. After direct substitution of Eqs. (A.3) and (A.4) into Eq. (A.2) we have

$$\mathcal{Z}_\nu(E_0;E,x)\,\psi_\nu(E_0;E,x) = \int_0^{y_0}\Phi_\nu(y,E)\,\psi_\nu(E_0;E_y,x)\,\mathrm{d}y. \tag{A.5}$$

Clearly, $\mathcal{Z}_\nu(E_0;E,x) \to 0$ and $\psi_\nu(E_0;E,x) \to x\Phi_\nu(0,E_0)/\lambda_\nu(E_0)$ as $E \to E_0$ for any x.

The new "Z factor", $\mathcal{Z}_\nu(E_0;E,x)$, can be found from Eqs. (A.3)–(A.5) by an iteration algorithm similar to the algorithm described in Section 2. Putting $\mathcal{Z}_\nu = 0$ as a zero approximation we have

$$\psi_\nu^{(0)}(E_0;E,x) = \frac{\Omega_\nu(E,E_0)}{\lambda_\nu(E)\,\mathcal{D}_\nu(E,E_0)}\left[\mathrm{e}^{x\mathcal{D}_\nu(E,E_0)} - 1\right] \tag{A.6}$$

and subsequently

$$\mathcal{Z}_\nu^{(1)}(E_0;E,x) = \int_0^{y_0}\Phi_\nu(y,E)\left[\frac{\psi_\nu^{(0)}(E_0;E_y,x)}{\psi_\nu^{(0)}(E_0;E,x)}\right]\mathrm{d}y. \tag{A.7}$$

The next steps of the algorithm are quite obvious; so there is no need to write out the corresponding cumbersome formulas here.

Let us briefly sketch the leading approximations for ψ_ν and $\mathcal{Z}_\nu$, since they contain the main features of the exact solution. As is seen from Eq. (A.6), for every $E < E_0$ there is a depth,

$$x_*(E_0,E) = \frac{1}{\mathcal{D}_\nu(E,E_0)}\ln\frac{\lambda_\nu(E)}{\lambda_\nu(E_0)},$$

at which the flux of neutrinos of energy E reaches the maximum. Function $x_*(E_0,E)$ increases when E decreases and tends to the minimum, $\lambda_\nu(E_0)$, as $E \to E_0$. At any finite depth, secondary neutrinos "remember" about their “parents” (the E_0 dependence does not disappear with increasing depth). Due to the nontrivial shape of the regeneration function Φ_ν (see Fig. 2), the spectrum of secondary neutrinos is rather complex and transforms drastically with depth.

For $x \ll \lambda(E_0)$, the function $\psi_\nu^{(0)}$ behaves as $x\Omega_\nu(E,E_0)/\lambda_\nu(E)$. Therefore

$$\mathcal{Z}_\nu^{(1)}(E_0;E,0) = \int_0^{y_0} \Phi_\nu(y,E)\left[\frac{\Omega_\nu(E_y,E_0)\,\lambda_\nu(E)}{\Omega_\nu(E,E_0)\,\lambda_\nu(E_y)}\right] \mathrm{d}y.$$

Taking into account that $\lambda_\nu(E) > \lambda_\nu(E_0)$ for $E < E_0$ (see footnote 8), we get the asymptotic behaviour of $\mathcal{Z}_\nu^{(1)}$ for $x \to \infty$:

$$\mathcal{Z}_\nu^{(1)}(E_0;E,x) \sim \int_0^{y_0} \Phi_\nu(y,E)\left[\frac{\Omega_\nu(E_y,E_0)}{\Omega_\nu(E,E_0)}\right]\left[\frac{\lambda_\nu(E)-\lambda_\nu(E_0)}{\lambda_\nu(E_y)-\lambda_\nu(E_0)}\right] \exp[-x\mathcal{D}_\nu(E,E_y)]\,\mathrm{d}y \to 0.$$

With the function $\psi_\nu(E_0;E,x)$ in hand, we can obtain the solution to the transport Eq. (2) for *any* initial spectrum $F_\nu^0(E)$. Indeed, multiplying Eq. (A.1) by $F_\nu^0(E_0)$ and integrating over E_0, we have

$$\begin{aligned} F_\nu(E,x) &= \int_0^\infty F_\nu^0(E_0)\,G_\nu(E_0;E,x)\,\mathrm{d}E_0 \\ &= F_\nu^0(E)\,\mathrm{e}^{-x/\lambda_\nu(E)} + \int_E^\infty F_\nu^0(E_0)\,\psi_\nu(E_0;E,x)\,\mathrm{e}^{-x/\lambda_\nu(E_0)}\,\frac{\mathrm{d}E_0}{E}. \end{aligned} \tag{A.8}$$

The first term on the right side of Eq. (A.8) describes neutrino absorption and the second one the neutrino regeneration due to energy loss through the reactions $\nu T \to \nu X$. Eq. (A.8) is in fact equivalent to Eq. (3) but, when the function $\psi_\nu(E_0;E,x)$ is known, Eq. (A.8) becomes much more convenient for calculations because ψ_ν is independent from the initial spectrum[10]. Due to the mentioned equivalence, we can get a useful representation for the Z factor in terms of the function ψ_ν:

$$Z_\nu(E,x) = \frac{\lambda_\nu(E)}{x}\ln\left[1+\int_0^1 \eta_\nu(y,E)\,\psi_\nu(E_y;E,x)\,\mathrm{e}^{-x\mathcal{D}_\nu(E,E_y)}\,\frac{\mathrm{d}y}{1-y}\right]. \tag{A.9}$$

It should be noted that the Z factor calculated in the nth approximation using the algorithm (6)–(7) agrees only numerically rather than analytically with that calculated from Eq. (A.9), employing the iteration algorithm for ψ_ν. In particular, substituting $\psi_\nu = \psi_\nu^{(0)}$ into Eq. (A.9) yields

$$Z_\nu(E,x) = \frac{\lambda_\nu(E)}{x}\ln\left[1+\frac{xZ_\nu^{(1)}(E,x)}{\lambda_\nu(E)}\right] \equiv Z_\nu^{(\mathrm{I})}(E,x),$$

where $Z_\nu^{(1)}(E,x)$ is defined by Eq. (9). Thus

$$Z_\nu^{(\mathrm{I})}(E,x) = Z_\nu^{(1)}(E,x)\left[1-\frac{xZ_\nu^{(1)}(E,x)}{2\lambda_\nu(E)}+\ldots\right] \leqslant Z_\nu^{(1)}(E,x).$$

[10] However, Eq. (A.8) has one evident technical drawback. To use it, one must calculate 3-dimensional arrays that are hard to interpolate due to the very strong dependence of ψ_ν and $\mathcal{Z}_\nu$ from their arguments. From this point of view, the algorithm described in Section 2 is of course simpler.

However, the $Z_\nu^{(\mathrm{I})}(E,x)$ can be approximated by $Z_\nu^{(1)}(E,x)$ with a very good accuracy because $xZ_\nu^{(1)}(E,x)/\lambda_\nu(E) \ll 1$ in most cases of interest for neutrino astrophysics.

Appendix B. Neutrino transport equation with a source function

Here, we briefly show how to take into account contributions from production of neutrinos through reactions $\nu_\ell T \to \nu_{\ell'} X$ $(\ell \neq \ell')$ or through the reaction chains mentioned in the introduction in the case when these contributions may be treated as corrections to the principal solution described in Section 2 and Appendix A. Clearly, the problem reduces to the transport equation (2) with a source function $S_\nu(E,x)$ on the right side. In line with our general approach, we will seek the solution to this equation in the following form [11]:

$$F_S(E,x) = \int_0^x S_\nu(E,x') \exp\left[-\int_{x'}^x \frac{1-\mathcal{Z}_\nu(E,x'')}{\lambda_\nu(E)}\,\mathrm{d}x''\right]\mathrm{d}x', \tag{B.1}$$

with $\mathcal{Z}_\nu(E,x)$ a positive function satisfying the equation

$$\mathcal{Z}_\nu(E,x) = \int_0^1 \eta_S(y,E;x)\,\Phi_\nu(y,E)\,\mathrm{d}y, \tag{B.2}$$

where we introduced

$$\eta_S(y,E;x) = \frac{F_S(E_y,x)}{F_S(E,x)\,(1-y)}.$$

It is easy to verify that $F_S(E,x) \sim xS_\nu(E,0)$ as $x \to 0$. Therefore,

$$\eta_S(y,E;0) = \frac{S_\nu(E_y,0)}{S_\nu(E,0)\,(1-y)},$$

and this function is assumed to be finite for any E and y.

The algorithm for the solution to Eqs. (B.1), (B.2) is quite obvious: putting $\mathcal{Z}_\nu^{(0)} = 0$ yields

$$F_S^{(0)}(E,x) = \int_0^x S_\nu(E,x-x')\,\mathrm{e}^{-x'/\lambda_\nu(E)}\,\mathrm{d}x', \qquad \mathcal{Z}_\nu^{(1)}(E,x) = \int_0^1 \eta_S^{(0)}(y,E;x)\,\Phi_\nu(y,E)\,\mathrm{d}y,$$

etc. The formal question about the finiteness of the involved integrals over y is closely related to the very difficult problem of the asymptotic behaviour for the νN inclusive and total cross sections as $E \to \infty$. This problem is beyond the scope of this study, but we can avoid it introducing a cutoff $y_0 = 1 - E/E_0$ (with $E_0 \gg E$) as the upper limit of the integrals. The reason for such a cutoff is in the fact that any physical source function, $S_\nu(E,x)$, must exponentially vanish as $E \to \infty$ (cf. footnote 7).

References

[1] E. Roulet, Phys. Rev. D 47 (1993) 5247;
D. Fargion and A. Salis, in: Proc. 25th Int. Cosmic Ray Conf., Durban, 1997, eds. M.S. Potgieter et al. (Wesprint, Potchefstroom, 1997), Vol. 7, p. 154;

[11] We suppose $F_S(E,0) = 0$ as the boundary condition.

D. Fargion, B. Mele and A. Salis, preprint astro-ph/9710029 (October, 1997);
T.J. Weiler, preprint hep-ph/9710431 (October, 1997); Astropart. Phys., in press;
E. Waxman, preprint astro-ph/9804023 (April, 1998); Astropart. Phys., submitted.

[2] S.W. Barwick (for the AMANDA Collaboration), in: Proc. 25th Int. Cosmic Ray Conf. Durban, 1997, eds. M.S. Potgieter et al. (Wesprint, Potchefstroom, 1997), Vol. 7, p. 1;
N. de Botton (for the ANTARES Collaboration), in: Proc. 25th Int. Cosmic Ray Conf. Durban, 1997, eds. M.S. Potgieter et al. (Wesprint, Potchefstroom, 1997), Vol. 7, p. 17;
L.A. Kuzmichev (for the Baikal Collaboration), in: Proc. 25th Int. Cosmic Ray Conf. Durban, 1997, eds. M.S. Potgieter et al. (Wesprint, Potchefstroom, 1997), Vol. 7, p. 21;
A. Capone (for the NESTOR Collaboration), in: Proc. 25th Int. Cosmic Ray Conf. Durban, 1997, eds. M.S. Potgieter et al. (Wesprint, Potchefstroom, 1997), Vol. 7, p. 49.

[3] V.S. Berezinsky, S.V. Bulanov, V.A. Dogiel, V.L. Ginzburg, V.S. Ptuskin, Astrophysics of Cosmic Rays, ed. V.L. Ginzburg (North-Holland, Amsterdam, 1990).

[4] J.G. Learned, Phil. Trans. Roy. Soc. London A 346 (1994) 99;
T.K. Gaisser, F. Halzen and T. Stanev, Phys. Rep. 258 (1995) 173;
F. Halzen, Comments Nucl. Part. Phys. 22 (1997) 155.

[5] A.L. Provorov and I.M. Zheleznykh, Astropart. Phys. 4 (1995) 55;
G.M. Frichter, J.P. Ralston and D.W. McKay, Phys. Rev. D 53 (1996) 1684;
L.G. Dedenko et al., preprint astro-ph/9705189 (May, 1997), and references therein.

[6] K.S. Capelle, J.W. Cronin, G. Parente and E. Zas, Astropart. Phys. 8 (1998) 321.

[7] M. Boratav (for the Auger Collaboration), in: Proc. 25th Int. Cosmic Ray Conf. Durban, 1997, eds. M.S. Potgieter et al. (Wesprint, Potchefstroom, 1997), Vol. 5, p. 205.

[8] J. Linsley, in: Proc. 19th Int. Cosmic Ray Conf., La Jolla, CA, 1985, eds. F.C. Jones et al. (NASA, Washington, DC, 1985), Vol. 3, p. 438;
Y. Takahashi, in: Proc. 24th Int. Cosmic Ray Conf., Roma, 1995, Vol. 3, p. 595;
J.F. Ormes, et al. (OWL Collaboration), in: Proc. 25th Int. Cosmic Ray Conf. Durban, 1997, eds. M.S. Potgieter et al. (Wesprint, Potchefstroom, 1997), Vol. 5, p. 273;
J. Linsley, L. Scarsi, P. Spillantini and Y. Takahashi, in: Proc. 25th Int. Cosmic Ray Conf. Durban, 1997, eds. M.S. Potgieter et al. (Wesprint, Potchefstroom, 1997), Vol. 5, p. 385;
P. Attinà, et al., in: Proc. 25th Int. Cosmic Ray Conf. Durban, 1997, M.S. Potgieter et al. (Wesprint, Potchefstroom, 1997), Vol. 5, p. 389;
C.N. De Marzo (for the Airwatch Collaboration), preprint physics/9712039 (December, 1997), to appear in: Proc. 5th Int. Workshop on "Topics in Astroparticle and Underground Physics" (TAUP'97), LNGS, Assergi, 1997.

[9] J. Linsley, in: Proc. 25th Int. Cosmic Ray Conf. Durban, 1997, eds. M.S. Potgieter et al. (Wesprint, Potchefstroom, 1997), Vol. 5, p. 381, and references therein.

[10] V.S. Berezinsky, A.G. Gazizov, G.T. Zatsepin and I.L. Rozental', Yad. Fiz. 43 (1986) 637 [Sov. J. Nucl. Phys. 43 (1986) 406].

[11] E.V. Bugaev, S.P. Mikheyev and O.V. Suvorova, in: Proc. 24th Int. Cosmic Ray Conf., Roma, 1995, Vol. 1, p. 666.

[12] A. Nicolaidis and A. Taramopoulos, Phys. Lett. B 386 (1996) 211.

[13] V.A. Naumov, S.I. Sinegovsky and E.V. Bugaev, Yad. Fiz. 57 (1994) 439 [Phys. Atomic Nucl. 57 (1994) 412].

[14] V.A. Naumov and T.S. Sinegovskaya, in preparation.

[15] K.S. Thorne and A.N. Żytkow, Ap. J. 212 (1977) 832.

[16] F. Halzen and D. Saltzberg, Phys. Rev. Lett. 81 (1998) 4305.

[17] J.G. Learned and S. Pakvasa, Astropart. Phys. 3 (1995) 267.
D. Fargion, preprint astro-ph/9704205.

[18] R. Gandhi, C. Quigg, M. Reno and I. Sarcevic, Astropart. Phys. 5 (1996) 81.

[19] R. Gandhi, C. Quigg, M. Reno and I. Sarcevic, Phys. Rev. D 58 (1998) 093009.

[20] H. Plothow-Besch, "PDFLIB: Nucleon, Pion and Photon Parton Density Functions and α_s Calculations", User's Manual – Version 7.09, W5051 PDFLIB, CERN-PPE report 1997.07.02; Comput. Phys. Comm. 75 (1993) 396; Int. J. Mod. Phys. A 10 (1995) 2901.

[21] H.L. Lai et al. (CTEQ Collaboration), Phys. Rev. D 51 (1995) 4763.

[22] G. Sigl, Phys. Rev. D 57 (1998) 3786.

[23] R.M. Barnett et al. (Particle Data Group), Phys. Rev. D 54 (1996) 1.

[24] V.A. Naumov, T.S. Sinegovskaya, S.I. Sinegovsky, Nuovo Cim. A 111 (1998) 129.